Chiral and Collinear Ordering in a Distorted Triangular Antiferromagnet

A. I. Smirnov,[1] L. E. Svistov,[1] L. A. Prozorova,[1] A. Zheludev,[2] M. D. Lumsden,[2] E. Ressouche,[3] O. A. Petrenko,[4] K. Nishikawa,[5,*] S. Kimura,[5] M. Hagiwara,[5] K. Kindo,[6] A. Ya. Shapiro,[7] and L. N. Demianets[7]

[1]*P. L. Kapitza Institute for Physical Problems RAS, 119334 Moscow, Russia*
[2]*Neutron Scattering Science Division, Oak Ridge National Laboratory, Oak Ridge, Tennessee 37831-6393, USA*
[3]*CEA-Grenoble, DRFMC-SPSMS-MDN, 17 rue des Martyrs, 38054 Grenoble Cedex 9, France*
[4]*Department of Physics, University of Warwick, Coventry, CV4 7AL, United Kingdom*
[5]*Center for Quantum Science and Technology under Extreme Conditions (KYOKUGEN), Osaka University, 1-3 Machikaneyama, Toyonaka, Osaka 560-8531, Japan*
[6]*Institute for Solid State Physics (ISSP), University of Tokyo, 5-1-5 Kashiwanoha, Kashiwa, Chiba 277-8581, Japan*
[7]*A. V. Shubnikov Institute for Crystallography RAS, 117333 Moscow, Russia*

(Received 17 July 2008; published 21 January 2009)

Magnetization, specific heat, and neutron diffraction measurements are used to map out the entire magnetic phase diagram of $KFe(MoO_4)_2$. This stacked triangular antiferromagnet is structurally similar to the famous multiferroic system $RbFe(MoO_4)_2$. Because of an additional small crystallographic distortion, it contains two sets of inequivalent distorted magnetic triangular lattices. As a result, the spin network breaks down into two intercalated yet almost independent magnetic subsystems. One is a collinear antiferromagnet that shows a simple spin-flop behavior in applied magnetic fields. The other is a helimagnet that instead goes through a series of exotic commensurate-incommensurate phase transformations. In the various phases one observes either true three-dimensional or unconventional quasi-two-dimensional ordering.

DOI: 10.1103/PhysRevLett.102.037202 PACS numbers: 75.25.+z, 75.30.Kz, 75.40.Cx, 75.50.Ee

The control of electric properties by an applied magnetic field is of intense interest for both applications and fundamental reasons and has fueled considerable interest in multiferroic materials. Such control has proven challenging as the symmetries of magnetic and electric degrees of freedom are often mutually exclusive [1]. In recent years, a new class of materials has been discovered in which ferroelectric and magnetic phase transitions occur simultaneously [2–7]. In these chiral magnets, the magnetically ordered states break inversion symmetry allowing ferroelectricity.

A spectacular example of such behavior was recently found in the layered molybdenate $RbFe(MoO_4)_2$ [8]. The geometric frustration of magnetic interactions in this triangular-lattice antiferromagnet (TLAFM) is resolved through a helimagnetic ''120°'' spin ordering in each triangular plane of $S = 5/2$ Fe^{3+} ions [9,10]. Understanding the physics of that material required a mapping of its magnetic phase diagram. In particular, it was found that an applied magnetic field disrupts the chiral state, thus destroying ferroelectricity. In this work we decipher the magnetic phase diagram of the structurally very similar compound $KFe(MoO_4)_2$. Using a combination of experimental techniques, we uncover qualitatively different and considerably more complex behavior than in $RbFe(MoO_4)_2$. We observe collinear and helical, commensurate and incommensurate structures that are ordered in either three or two dimensions and reside *simultaneously and independently* on alternating intercalated magnetic layers. Such peculiar ordering is not known in any other TLAFM materials. It underscores the proximity of multiple competing ground states in this class of geometrically frustrated magnets (see, for example, Ref. [11]), and has direct implications for the potential multiferroic effect in $KFe(MoO_4)_2$.

The only structural difference between the two materials is tiny crystallographic distortion found in $KFe(MoO_4)_2$. As in $RbFe(MoO_4)_2$, at high temperatures the spin network in $KFe(MoO_4)_2$ is a perfect triangular lattice (space group D_{3d}^3) $a = 5.66$ Å and $c = 7.12$ Å. Distortions occur due to phase transitions at 311 and 139 K (see, e.g., [12,13]). The low-temperature phase has a doubled period c and is monoclinic (group C_{2h}^3). Fe plane becomes a *distorted* triangular lattice with two unequal exchange constants J_1 and J_2 (Fig. 1). Moreover, the adjacent Fe layers become crystallographically inequivalent, with exchange constants J_1' and J_2'. The actual lattice distortion is too small to be detected in neutron diffraction experiments, and we shall henceforth adopt a hexagonal lattice notation. This said, magnetic systems with geometric frustration can be extraordinarily sensitive to even the smallest lattice effects. Recent examples include the ''spin-Peierls-like'' ordering in the spinel $ZnCr_2O4$ [14] and the peculiar vortexlike structure in UNi_4B [15] For $KFe(MoO_4)_2$, a previous ESR study [16] came to a seemingly paradoxical conclusion: at low temperatures, in zero magnetic field, a helical spin structure coexists with a collinear state. Based on a theoretical study of the distorted TLAFM model [17], it was hypothesized that the two types of magnetic order reside almost independently in the two

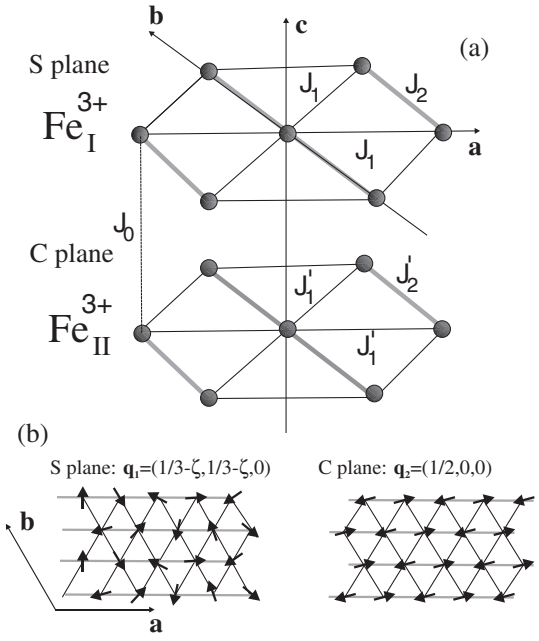

FIG. 1. (a) Arrangement of magnetic ions in the crystal structure of $KFe(MoO_4)_2$ showing two inequivalent Fe^{3+} planes. (b) Schematic representation of the zero-field magnetic structure.

inequivalent types of distorted triangular spin lattices, referred to as "*S* layers" and "*C* layers," respectively.

To verify this bold assumption we performed magnetic neutron diffraction experiments using single-crystal samples from the same batch [16]. The crystals are transparent thin plates, typically 1–5 mg, with the cleavage planes perpendicular to the threefold axis. The data were taken on the HB-1 and HB-1A three-axis spectrometers at ORNL operating in two-axis mode, using a pyrolitic graphite PG(002) monochromator to select $\lambda = 2.46$ Å for HB-1 and $\lambda = 2.37$ Å for HB-1A. At low temperatures, two sets of magnetic Bragg peaks emerge, with propagation vectors $(1/3 - \zeta, 1/3 - \zeta, 0)$, $\zeta = 0.038$, and $(1/2, 0, 0)$, respectively. The observed ordering temperatures for the two sets of reflections are identical within experimental accuracy: $T_N = 2.4$ K. An analysis of 19 inequivalent Bragg reflections in the $(h, k, 0)$ plane at $T = 1.5$ K revealed that the $(1/3 - \zeta, 1/3 - \zeta, 0)$ peaks can be entirely accounted for by a planar helimagnetic state, with spins rotating in the (a, b) plane. The 14 inequivalent sets of $(1/2, 0, 0)$-type Bragg intensities measured in the $(h, k, 0)$ plane are consistent with a collinear AFM spin arrangement, with spins in the (a, b) plane and forming a small angle of 15° with the a axis. Thus the diffraction data confirm the two-layer model. As discussed in Ref. [16], the drastically different spin arrangement in *C* and *S* layers can be accounted for by the difference in the ratios $R = J_1/J_2$ vs $R' = J'_1/J'_2$: theory predicts a switch from a helimagnetic state with $\cos[2\pi(1/3 - \zeta)] = -J_1/2J_2$ for $R < 2$ to a collinear state at $R > 2$ [17].

The complexity of the H-T phase diagram of $KFe(MoO_4)_2$ was revealed in bulk measurements. Steady-state magnetization up to 12 T applied field and specific heat data were collected using a vibrating sample magnetometer and commercial Quantum Design PPMS calorimeter, respectively. High-field magnetization data were taken in the fields up to 25 T using a pulsed magnet at the KYOKUGEN center at Osaka University. Typical experimental $C(T)$ and dM/dH curves are shown in Fig. 2. The lattice contribution to $C(T)$ can safely be assumed negligible in the relevant temperature range [18]. In zero field, we observe a sharp specific heat anomaly at $T_1 = 2.5$ K [Fig. 2(b)]. In a magnetic field applied in the (a, b) plane this anomaly shifts to lower temperatures and survives up to $H = 5$ T. For $H > 2$ T an additional peak is observed at $T_2 > T_1$. Beyond $H > 5$ T the T_1 anomaly is replaced by a new feature at T_3. The latter also moves to lower temperatures with increasing field. Yet another maximum in specific heat is observed at $T_4 < T_2$ in the high field regime. For a field applied along the c axis, the only observed feature is saturation at $H_{\text{sat}\|} = 16.9$ T. However, for a field in the (a, b) plane, the magnetization curves show four distinct anomalies. A jump of dM/dH at

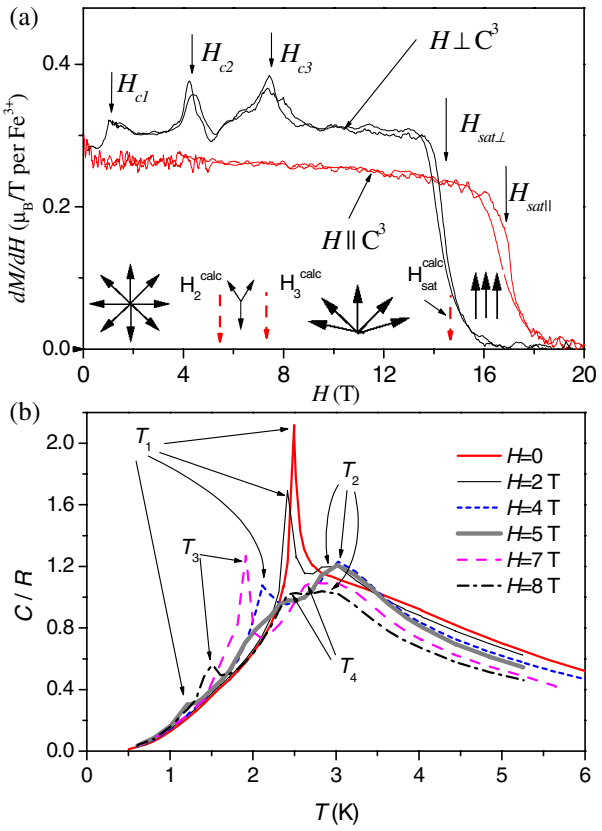

FIG. 2 (color online). (a) Field derivative of the magnetization measured at $T = 1.6$ K. Solid arrows are experimentally observed anomalies. Dashed arrows and spin diagrams are explained in the text. (b) Specific heat measured on a 1 mg $KFe(MoO_4)_2$ single-crystal sample in magnetic fields applied in the (a, b) plane.

$H_1 \sim 1.2$ T is followed by sharp maxima at $H_2 \simeq 4.5$ T and $H_3 \simeq 7.5$ T. Finally, a saturation is reached at $H_{\mathrm{sat}\perp} = 14.5$ T. Some samples show an additional smeared peak in dM/dH in the field range above 8 T in the temperature interval $2 < T < 2.5$ K. These results, together with the $M(T)$ data from Ref. [16], allow us to reconstruct the entire H-T phase diagram, as shown in Fig. 3.

The propagation vectors in the various phases were determined in neutron experiments on the D23 lifting-counter diffractometer at ILL (Grenoble) using $\lambda = 2.38$ Å neutrons. The field was applied along the b axis. Typical measured field dependencies of Bragg intensities are shown in Fig. 4. At $T = 100$ mK the intensities of commensurate $(1/2, 0, 0)$-type peaks go through two consecutive jumps at $H_1 = 1.3$ T and $H_1' = 2.1$ T. These transitions seem to have no effect on the incommensurate reflections. At $T = 1.5$ K a single intensity jump is detected at $H_1 = 1$ T. As previously discussed in [16], the transition is to be associated with a spin flop in the C planes. The additional transition seen at low temperature at H_1' requires further investigation. At higher fields all the action occurs within the S planes. The intensity of the incommensurate $(1/3 - \zeta, 1/3 - \zeta, 0)$-type reflections decreases and vanishes beyond $H_2 \sim 4$ T. Within experimental resolution the value of the magnetic propagation vector is field independent. Beyond H_2 the $(1/3 - \zeta, 1/3 - \zeta, 0)$-type peaks are replaced by *commensurate* reflections of type $(1/3, 1/3, 0)$. The latter first increases in intensity, peaks at around 6 T, and decreases at higher fields to vanish at $H_3 \sim 8$–9 T. At still higher fields, no magnetic reflections were found on either the $(h, h, 0)$, $(1/3 - \zeta, 1/3 - \zeta, l)$, or $(1/3, 1/3, l)$ reciprocal-space rods. At the temperature of neutron measurements ($T = 100$ mK and $T = 1.5$ K) we found no signature of a high-field transition that could be associated with the T_4-anomaly described above.

A remarkable feature of the neutron data is the different dimensionality of magnetic ordering in the different phases. Scans across the $(1/2, 0, 0)$-type and $(1/3 - \zeta, 1/3 - \zeta, 0)$ − type reflections are resolution-limited along the h, k, and l directions. In contrast, the $(1/3, 1/3, 0)$-type peaks in the regime $H_2 < H < H_3$ are actually Bragg rods parallel to the c axis, stretching across much of the Brillouin zone in the l directions. The corresponding c-axis correlation length is only six lattice units, while that in the (a, b) plane is about 100 lattice units. The transition to the short range ordered state at T_2 corresponds to a smeared $C(T)$ anomaly in contrast to a sharp peak at the 3D transition at T_1.

Because of the stringent geometric restrictions imposed by the cryomagnet in the lifting-counter geometry, at $H > 0$ it was not possible to collect enough diffraction data for even a semiquantitative structure analysis. Instead, guidance to understanding the complex phases realized in the S planes can be drawn from the theoretical

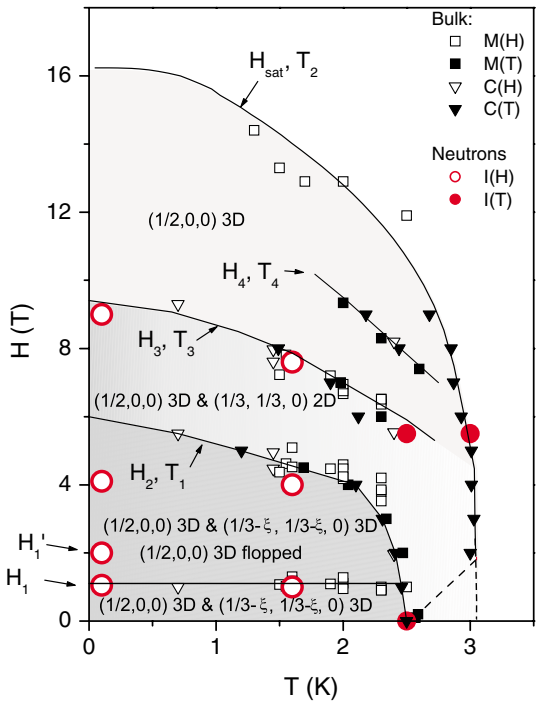

FIG. 3 (color online). Cumulative magnetic phase diagram of $KFe(MoO_4)_2$ for a magnetic field applied in the (a, b) plane.

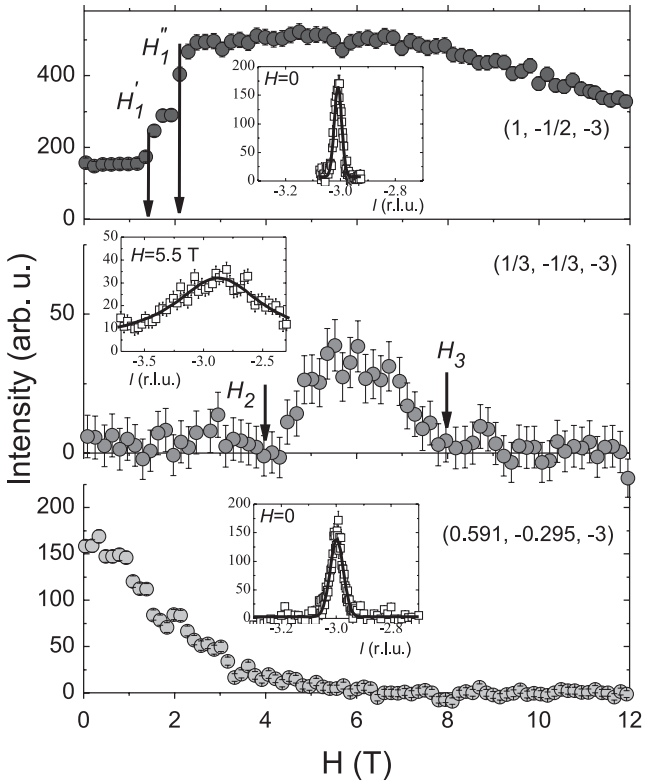

FIG. 4. Upper and lower panels: Field dependencies of magnetic Bragg intensities measured in $KFe(MoO_4)_2$ at $T = 100$ mK. Middle panel: Field dependencies of magnetic Bragg intensities at $T = 1.5$ K. Insets: Typical l scans measured across the corresponding reflections.

work of Ref. [17]. First, we can estimate the relevant exchange parameters from the saturation fields and susceptibility. Since all neutron reflections observed in high fields correspond to C planes, we assume that it is these planes that are involved in saturation. The saturation fields are then given by $g\mu_B H_{\mathrm{sat}\perp} = 8(J_1' + J_2')S$ and $g\mu_B H_{\mathrm{sat}\parallel} = 8(J_1' + J_2')S + 2DS$, respectively, where D is the single-ion easy-plane anisotropy defined as in [10]. Using the observed values of $H_{\mathrm{sat}\perp}$ and $H_{\mathrm{sat}\parallel}$, we get $J_1' + J_2' = 0.96$ K and $D' = 0.32$ K. Beyond the spin flop at H_1, the contribution of C planes to magnetic susceptibility should be constant: $\chi_C = g^2\mu_B^2/[8(J_1' + J_2')]$. Subtracting this value from dM/dH data for $H_{c1} < H < H_{c2}$ we obtain the susceptibility of the S planes: $\chi_S \simeq 0.12\mu_B/\mathrm{T}$ per Fe^{3+} ion. Using the latter value and the measured $\zeta = 0.038$, by applying the equations in Ref. [17], we get $J_1 = 0.37$ K; $J_2 = 0.69$ K. As a self-consistency check, the experimental ratio $R = 0.53$ warrants a helimagnetic ground state for the S layers in zero field [17].

Now, the measured values ζ and $H_{\mathrm{sat}\perp}$ can be applied to reconstruct the phase transitions in the S planes. The critical fields $H_2^{\mathrm{calc}} = 5.7$ T, $H_3^{\mathrm{calc}} = 7.2$ T, calculated by use of ζ and H_{sat} following the theory [17], are shown in dashed lines in Fig. 2(a). As indicated by the arrow diagrams, and in perfect agreement with the diffraction experiments, at low fields one expects an incommensurate spiral structure confined to the (a, b) plane. Beyond the phase transition at H_2^{calc} the spins should form a commensurate three-sublattice configuration with the 2D propagation vector $(1/3, 1/3)$, as observed experimentally. At still higher fields, beyond H_3^{calc}, the incommensurate state is expected to be restored. The spins will form a fan-type structure, oscillating in a small angular interval, remaining within the (a, b) plane. Note that neutron diffraction failed to detect any incommensurate peaks beyond H_3^{calc}. This implies that either the system remains disordered or that the ordering vector is outside our search range in reciprocal space. A flop of the spin plane perpendicular to the field direction is expected [17] at $H = H_{sf} = 6.5$ T. Instead of this instability, we observe the suppression of the S plane Bragg peaks.

Even as the S planes go through a series of phase transitions in an applied field, the C planes remain unaffected, and vice versa, as if they were totally decoupled. At the same time, in zero field the ordering temperatures for the two wave vectors coincide, or, at least, are very close. Whether or not this is merely a coincidence is yet to be clarified.

The distortion of the triangular planes in $KFe(MoO_4)_2$ is minuscule, yet it has a profound effect on the magnetic structures. This is a vivid illustration of the fact that the ground states in frustrated magnets are selected among numerous energetically close competing states. Since the multiferroic properties are inherently connected to the symmetries of the magnetic structure, one can expect $KFe(MoO_4)_2$ to be qualitatively different in this respect from its Rb-based counterpart. Future magnetoelectric experiments should address this issue.

Research at ORNL was supported by the Scientific User Facilities Division, Office of Basic Energy Sciences, U.S. DOE. The work at Kapitza Institute is supported by the Russian Foundation for Basic Research. The work at Warwick University is supported by EPSRC grant. A. I. S. received support from the Foreign Visiting Professor Program in KYOKUGEN, Osaka University.

*Present address: Hitachi, Ltd., 890 Kashimada, Kawasaki, Kanagawa, 212-8567 Japan.

[1] S.-W. Cheong and M. Mostovoy, Nature Mater. **6**, 13 (2007).
[2] T. Kimura, T. Goto, H. Shintani, K. Ishizaka, T. Arima, and Y. Tokura, Nature (London) **426**, 55 (2003).
[3] M. Kenzelmann, A. B. Harris, S. Jonas, C. Broholm, J. Schefer, S. B. Kim, C. l. Zhang, S.-W. Scheong, O. P. Vajk, and J. W. Lynn, Phys. Rev. Lett. **95**, 087206 (2005).
[4] N. Hur, S. Park, P. A. Sharma, S. Guha, and S.-W. Cheong, Phys. Rev. Lett. **93**, 107207 (2004).
[5] L. C. Chapon, G. R. Blake, M. J. Gutmann, S. Park, N. Hur, P. G. Radaelli, and S.-W. Cheong, Phys. Rev. Lett. **93**, 177402 (2004).
[6] T. Kimura, G. Lawes, and A. P. Ramirez, Phys. Rev. Lett. **94**, 137201 (2005).
[7] G. Lawes, A. B. Harris, T. Kimura, N. Rogado, R. J. Cava, A. Aharony, O. Entin-Wohlman, T. Yildrim, M. Kenzelmann, C. Broholm, and A. P. Ramirez, Phys. Rev. Lett. **95**, 087205 (2005).
[8] M. Kenzelmann, G. Lawes, A. B. Harris, G. Gasparovic, C. Broholm, A. P. Ramirez, G. A. Jorge, M. Jaime, S. Park, Q. Huang, A. Ya. Shapiro, and L. A. Demianets, Phys. Rev. Lett. **98**, 267205 (2007).
[9] A. I. Smirnov, H. Yashiro, S. Kimura, M. Hagiwara, Y. Narumi, K. Kindo, A. Kikkawa, K. Katsumata, A. Ya. Shapiro, and L. N. Demianets, Phys. Rev. B **75**, 134412 (2007).
[10] L. E. Svistov, A. I. Smirnov, L. A. Prozorova, O. A. Petrenko, L. N. Demianets, and A. Ya. Shapiro, Phys. Rev. B **67**, 094434 (2003).
[11] A. V. Chubukov and D. I. Golosov, J. Phys. Condens. Matter **3**, 69 (1991).
[12] A. I. Otko, N. M. Nesterenko, and L. V. Povstannyi, Phys. Status Solidi A **46**, 577 (1978).
[13] G. A. Smolenskii, I. G. Sinii, E. G. Kuzminov, and E. F. Dudnik, Izv. Akad. Nauk SSSR, Ser. Fiz. **43**, 1650 (1979).
[14] S.-H. Lee, C. Broholm, T. H. Kim, W. Ratcliff, II, and S-W. Cheong, Phys. Rev. Lett. **84**, 3718 (2000).
[15] S. A. M. Mentink, A. Drost, G. J. Nieuwenhuys, E. Frikkee, A. A. Menovsky, and J. A. Mydosh, Phys. Rev. Lett. **73**, 1031 (1994).
[16] L. E. Svistov, A. I. Smirnov, L. A. Prozorova, O. A. Petrenko, A. Ya. Shapiro, and L. N. Dem'yanets, JETP Lett. **80**, 204 (2004).
[17] T. Nagamiya, K. Nagata, and Y. Kitano, Prog. Theor. Phys. **27**, 1253 (1962).
[18] L. E. Svistov, A. I. Smirnov, L. A. Prozorova, O. A. Petrenko, A. Micheler, N. Büttgen, A. Ya. Shapiro, and L. N. Demianets, Phys. Rev. B **74**, 024412 (2006).